Spectral and phase-amplitude coupling signatures in human deep brain oscillations during propofol-induced anaesthesia

Y.H. [1], D.W.[1], N.F.A.B.[2], S.W.[3], J.H.[1,2], S.Y.[4], J.J.F.[1], T.Z.A.[1], A.L.G.[1,*]

[1] Nuffield Department of Surgical Sciences, University of Oxford, John Radcliffe Hospital, Oxford OX3 9DU, UK

[2] Department of Physiology, Anatomy and Genetics, University of Oxford, Oxford OX1 3QX, UK

[3] Institute of Science and Technology for Brain-Inspired Intelligence, Fudan University, Shanghai 200433, China

[4] Nuffield Department of Anaesthesia, University of Oxford, John Radcliffe Hospital, Oxford OX3 9DU, UK

[*] Correspondence: alex.green@nds.ox.ac.uk

Abstract

Background: Both cortex and subcortical structures play important roles in alteration of consciousness. Some evidence points to general anaesthesia-induced unconsciousness being associated with distinct patterns of superficial cortical electrophysiological oscillations, but how general anaesthetics influence the deep brain neural oscillations and the interactions between the oscillations in humans is poorly understood.

Methods: Local field potentials (LFPs) were recorded in discrete deep brain regions, including anterior cingulate cortex (ACC), sensory thalamus, and periaqueductal grey (PAG) in humans during induction of unconsciousness with propofol. Power-frequency spectra, phase-amplitude coupling, coherence and directed functional connectivity analysis were used to characterize the LFPs in the awake and loss of consciousness states.

Results: An increase in alpha (7-13 Hz) power and decrease in gamma (30-90 Hz) power were observed in both deep cortical (ACC) and subcortical (sensory thalamus, PAG) areas during propofol-induced unconsciousness. A robust alpha-low gamma (30-60 Hz) phase-amplitude coupling induced by general anaesthesia was observed in ACC but not other regions studied. Moreover, alpha oscillations during unconsciousness were highly coherent within ACC and this rhythm exhibited a bidirectional information flow between left and right ACC but stronger left-to-right flow.

Conclusion: propofol elevates alpha oscillations and attenuates gamma oscillations in both cortical and subcortical areas. The alpha-gamma phase-amplitude coupling and the functional connectivity of alpha oscillations in ACC could be specific markers for loss of consciousness.

Keywords: anaesthesia; local field potential; anterior cingulate cortex; thalamus; periaqueductal grey

Introduction

How general anaesthesia (GA) causes unconsciousness and alterations in brain networks remains elusive. Functional imaging studies have identified changes of activities within several regions such as cortex, thalamus and brainstem during the transition to loss of consciousness (LOC) [1-3],

and the disruption of communication between these structures is thought to underlie LOC [3, 4]. Electrophysiological techniques, especially scalp electroencephalogram (EEG), are feasible for monitoring dynamic brain states under GA. EEG studies in humans show that propofol-induced LOC is accompanied by changes in EEG power across a broad range of frequencies, including an increase in global slow-wave (< 1 Hz) power [5, 6], increase in frontal alpha (8-14 Hz) power [6-8], and a decrease in occipital alpha power [6]. Similar patterns have been observed by using intracranial electrocorticography (ECoG) in humans during propofol-induced LOC [9, 10]. Different frequency oscillations are thought to represent different neural sources, for instance, low frequency oscillations appear to represent large scale cortical-subcortical interactions, e.g. thalamocortical circuits [11, 12], whereas higher frequency oscillations are locally generated and more likely to reflect local cell assembly organization [13, 14]. EEG and ECoG studies have identified distinct characteristics in low and high frequency oscillations during GA, suggesting both cortex and subcortical regions could play an important role in propofol-induced LOC. However, as neither EEG nor ECoG directly measures subcortical activity, any conclusions drawn using cortical recordings are by inference. Deep intracranial recordings in humans are required to investigate this fully.

In addition, most oscillations studies to date have treated each rhythm independently, offering limited insight into the modulation of brain network activity as a whole. Critical characteristics for understanding brain states related to consciousness may be contained in patterns of interactions between different frequencies that could be detected by cross-frequency coupling [15]. Cross-frequency coupling, more specifically phase-amplitude coupling (PAC), is believed to reflect neural coding and information processing within microscale and macroscale neural ensembles of the brain and play a role in regulation of neural networks during learning, memory, attention, and sensory processing [16-18]. Recent studies have found a variety of PAC characteristics related to anaesthesia [6, 9, 15, 19]. The coupling between the delta phase and gamma amplitude in cortex appears to strengthen with propofol-induced anaesthesia [9]. Different patterns of slow-wave (< 1 Hz) phase-alpha amplitude coupling were observed during propofol-induced anaesthesia [6, 15]. The influence of propofol on PAC of neural activities in deep cortical and subcortical areas in humans has not been clearly established.

To characterize the neural activities in deep brain regions and their interaction during anaesthesia, we measured local field potentials (LFPs) directly recorded from various brain areas, i.e. anterior cingulate cortex (ACC), sensory thalamus and periaqueductal grey (PAG), while administering propofol to patients undergoing deep brain stimulation (DBS) used as a treatment for chronic pain. We firstly investigated the spectral properties in LFPs during induction of GA with propofol using power spectral and time-frequency analysis. Furthermore, to investigate the interactions between different frequencies, we analysed the PAC characteristics in these regions. Moreover, we used coherence and directed transfer function analysis to assess the functional connectivity between areas for understanding the functional connection between different areas during anaesthesia.

Methods

Subjects

This study was conducted at the John Radcliffe Hospital, Oxford and approved by the Local Ethics Committee. Informed written consent was obtained from all participants.

Six patients undergoing DBS for chronic pain participated. Two underwent bilateral implantation of electrodes into the ACC, three underwent unilateral implantation electrodes into both the sensory thalamus (ventroposterior thalamus) and PAG, and one underwent unilateral implantation into sensory thalamus (Table 1).

The surgical procedure has been previously described [20, 21]. Medtronic 3387 electrodes with four active contacts (10.5 mm active, 1.5 mm × 4 contacts with 1.5 mm × 3 intervals) were implanted. Electrode implantation was performed under local anaesthesia (for sensory thalamus and PAG) or general anaesthesia (for ACC). The final electrode localization was confirmed for all patients on fused imaging of post-operative CT and pre-operative MRI. In all patients the electrodes were externalized for one week of trial stimulation to assess the degree of symptom relief. After the patients reported satisfactory relief following trial stimulation, they underwent the second stage operation to implant with a subcutaneous pulse generator under GA. Our experiment was performed during the second stage operation.

Anaesthetic procedures and data acquisition

The technique for induction of anaesthesia was at the discretion of the attending anaesthetist. In all cases, LOC was achieved by intravenous propofol (0.96-2 mg kg^{-1}) either by bolus injection or target-controlled infusion (target concentration 4-6 μg ml^{-1}). As is usual anesthetic practice, all patients also received intravenous opiates, either fentanyl (0.58 μg kg^{-1}; patient 2), alfentanil (6.67-15.5 μg kg^{-1}; patients 3 and 4) or remifentanil (target-controlled infusion at 6-8 ng ml^{-1}; patients 1, 5 and 6) before propofol. Standard monitoring techniques were employed, according to Association of Anaesthetists (GB and Ireland) guidelines. Time to LOC was determined by checking every 10 s for the loss of verbal response and eyelash reflex.

The LFPs in different brain regions including ACC, sensory thalamus and PAG were recorded from the implanted electrodes. Bipolar LFPs were recorded from three channels per electrode (0-1, 1-2, and 2-3: 0 being the deepest contact) with a common electrode placed on the surface of the mastoid. The LFPs were amplified using isolated CED 1902 amplifiers (×10,000, Cambridge Electronic Design, Cambridge, UK), filtered between 0.5 Hz and 500 Hz, and digitized using CED 1401 mark II at a sampling rate of 2048 Hz, displayed on-line and saved onto a hard disk using a custom-written program in Spike2 (Cambridge Electronic Design, Cambridge, UK).

Preprocessing

The LFPs data were bandpass filtered between 1 Hz and 90 Hz, notch filtered at 50 Hz, and down-sampled to 512 Hz. The data from each channel were visually inspected and those channels with noise or artifacts were excluded from further analysis (2 of 12 channels from ACC, 3 of 12 channels from sensory thalamus, and 2 of 9 channels from PAG).

Spectral analysis

After reviewing the recordings, two 60-s epochs of data were extracted for each patient in the awake and LOC states: (1) awake state, prior to propofol induction, and (2) LOC state, beginning at the 20 s after loss of eyelash reflex. The second epoch was chosen to ensure the patients were at LOC state in this time period.

Power spectra of the LFPs were calculated for all the patients in each state (awake, LOC) with the multitaper method using the Chronux toolbox [22, 23]. Multitaper parameters were set using time window lengths of T = 2 s, time-bandwidth product TW = 2, and number of tapers K = 3. The

dynamics of the LFPs during induction of general anaesthesia were studied by using multitaper spectrogram method with TW = 2, K = 3, and T = 2 s with 1.8 s overlap. The time-variant power in a frequency band of interest was computed by averaging the spectrogram over the frequency band. We computed the group-level time-variant powers in frequency bands by taking the mean across all patients with the data aligned to the induction of propofol and loss of eyelash reflex time points, respectively.

To characterize this changing frequency distribution over time during induction of GA quantitatively, the peak power and the frequency at the peak power at each time in spectrograms were extracted within a broad band of frequencies (e.g. between 6 Hz and 90 Hz) [24].

Cross-frequency coupling analysis

To detect the possible cross-frequency interactions between different frequency bands, the modulation index (MI) method [25, 26], which measured PAC between the phase of lower frequency (f_p) oscillations and the amplitude of higher frequency (f_A) oscillations, was employed in this study. To determine the frequency bands involved in PAC, a comodulogram plot was first constructed by representing the MI values of multiple (f_p,f_A) pairs on a color scale plot, with f_p filtered in 1-Hz steps with 2-Hz bandwidths and f_A in 2-Hz steps with 5-Hz bandwidths. To assess the statistical significance of the MI values, a surrogate data measure was performed. In this study, surrogate data was obtained by cutting either the phase or the amplitude time series into two blocks at a random time point and then exchanging the positions of the blocks [27]. This process destroys the specific cyclo-stationarities related to the hypothesized phase-amplitude relationship but only minimally interferes with the phase and amplitude dynamics of the original signal. We computed a distribution of 200 surrogate MI values for each pair of frequencies. Assuming that the surrogate MI values follow a normal distribution, we used a *p* value of 0.05 and applied the Bonferroni correction for multiple comparisons, only MI values with corresponding $p < 0.05$ were maintained for subsequent consideration. We computed the group-level MI in each frequency pair by taking the mean across all patients in awake and LOC states, respectively.

In the case of significant coupling, to characterize the coupling changes during induction of GA quantitatively, we computed the time-variant MI using a windowing approach with 15-s of sliding-window and 13-s of overlap. And the preferred phase of the coupling over time was determined by the phase of f_p at which the amplitude of f_A is highest in the phase-amplitude distribution.

Coherence analysis

The coherence between two LFPs signals was measured using a magnitude squared coherence estimate based on Welch's averaged periodogram method. The magnitude squared coherence estimate $C_{xy}(f)$ is the normalized cross-spectral density by the power spectral density with values between 0 and 1 that indicates the degree of covariability between signal x and y over different frequency ranges. In this study, the coherence was estimated by using multitaper methods with TW = 4, K = 7, and T = 4 s with 3 s overlap. A coherogram graphically illustrates coherence for different frequencies across time.

Directed transfer function (DTF) analysis

The directional functional connectivity between LFPs signals was measured by directed transfer function (DTF) [28], which is an approach for estimating causal interaction based on the multivariate autoregressive (MVAR) modelling:

$$\sum_{k=0}^{p} A_k X_{t-k} = E_t \quad (1)$$

where A_k are $N \times N$ matrices of model coefficients ($A_0 = I$), E_t is the vector of multivariate zero-mean uncorrelated white noise and p is the model order. To investigate the spectral properties, the above equation are transformed to the frequency domain:

$$X(f) = A^{-1}(f)E(f) = H(f)E(f) \quad (2)$$

where $H(f)$ is the inverse of the frequency-transformed coefficient matrix $A(f)$, and is defined as the transfer matrix of the system. In order to be able to compare the results obtained for different LFPs, here we used the normalization DTF that was performed by dividing each estimated inflow from channel j to i by all the inflows to channel i:

$$DTF_{ij}^2(f) = \frac{|H_{ij}(f)|^2}{\sum_{m=1}^{N}|H_{im}(f)|^2} \quad (3)$$

where $DTF_{ij}^2(f)$ is the normalized DTF from channel j to i with a value between 0 and 1. DTF analysis has been recently demonstrated to be a powerful and effective tool for evaluating both the direction and the strength of the directional influence between different neuronal activities [29, 30]. In this study, the DTF between multiple LFPs was evaluated using eConnectome toolbox [31].

A surrogate data measure was also used to assess the significance of the estimated DTF [32, 33]. In this method, the original time series were transformed to the Fourier space, in which the phases were randomly shuffled without changing the magnitude. The surrogate data in the Fourier space were then transformed back to the time domain. This process of phase shuffling preserves the spectral structure of the time series, which is suited for DTF analysis as both are measures of frequency-specific causal interactions. After shuffling, DTF estimation is applied to the surrogate data. The shuffling and DTF estimation procedures are repeated by a certain number of times (e.g. 200), we used a *p* value of 0.05 and only DTF values with corresponding $p < 0.05$ were maintained for subsequent consideration [33].

Group-level statistical analysis

Statistical significance of the differences of power in frequency bands and MI in frequency pairs between awake and LOC states were assessed. Due to the small number of patients, the comparisons were tentative while we used all LFP channels in each state to increase the sample size. Before comparison, raw values of power and MI in each state were examined for deviations from normality using the Kolmogorov–Smirnov test. The power and MI values were compared between awake and LOC states using the Wilcoxon signed ranks test if the data were not normally distributed or paired t-test. The signal processing was conducted using MATLAB (Version 9.1, MathWorks, Inc., Natick, MA, USA), and the statistical analysis was conducted using MATLAB and SPSS (Version 19, IBM, New York, NY, USA).

Results

LOC induces an increase in alpha band power and decrease in gamma band power

To reveal the dynamics of LFPs oscillations in ACC, sensory thalamus and PAG during induction of

GA, the spectrograms were computed. For descriptive purposes, representative results for each of the regions are provided from one patient with electrodes in ACC and one patient with electrodes in both sensory thalamus and PAG (Fig. 1A and B). The LFPs spectrograms showed changes during induction of GA with the most dominant characteristic being the increased power in alpha frequency band (7-13 Hz) in all three regions at the LOC state (Fig. 1A). The increase in power in delta band (1-3 Hz) in ACC and thalamus, and decrease in power in gamma band (30-90 Hz) in all three regions were also observed at the LOC state. There was an increase in power in the beta band (13-30 Hz) at ~30 s before LOC in ACC, and the broad-band beta power appeared to decrease its frequency and bandwidth toward the alpha band (Fig. 1A). To characterize this changing frequency distribution quantitatively, the peak power and frequency at the peak power within a broad band of frequencies (6-90 Hz) over time were estimated. The result showed that the peak frequency of the oscillations increased to irregular broad frequency ranges around 15-20 Hz (low beta band) in the transition period before LOC and then decreased to a regular narrow alpha frequency band around 9 Hz and remained stable at the LOC state in ACC, whereas these peak frequency changes did not appear in sensory thalamus and PAG (Fig. 1B). The increase in peak power appeared in all three regions at the LOC state (Fig.1 B).

Subsequently, the group-level time-variant powers in delta, alpha, low gamma (30-60 Hz) and high gamma (60-90 Hz) bands were computed by taking the mean across all patients with the data aligned to the time points of induction of propofol and loss of eyelash reflex, respectively (Fig.1 C). The group statistical analysis revealed that, compared to the awake state, there was a significant increase in power in the alpha band and decreases in both low gamma and high gamma bands in all regions during the propofol-induced LOC state (Fig. 1D). The delta power increased significantly in ACC and thalamus in the LOC state (Fig. 1D).

Alpha-gamma phase-amplitude coupling appears in ACC during LOC

The representative comodulograms in Figure 2 illustrated the PAC before and during the propofol-induced LOC state. An increase in alpha-low gamma PAC was observed in ACC in the LOC state compared to the awake state (Fig. 2A), and there was no significant PAC change between two states in both sensory thalamus and PAG (Fig. 2A). After averaging the PAC within the target frequency pair (alpha and low gamma) across all patients, statistical analysis showed that,

compared to the awake state, propofol induced a significant increase in alpha-low gamma PAC (p<0.05) in ACC (Fig. 2B).

The time-variant PAC was computed using a windowing approach. At the contacts with significant alpha-low gamma PAC, the magnitude of the alpha-low gamma PAC was temporally dynamic (Fig. 2C). Furthermore, the time-variant phase-amplitude distribution of the frequency pair showed that the preferred phase of the coupling shifted in the range of [π/2, π] with dynamic variation in the LOC state (Fig. 2D). The relationship between the temporally dynamic PAC and alpha power and low gamma power in ACC was analysed subsequently. The alpha-low gamma PAC was highly correlated with alpha power (Fig. 2E, $R^2 = 0.615,\ p = 1.22 \times 10^{-40}$), while the correlation with low gamma power was not significant (Fig. 2F, $R^2 = 0.003,\ p = 0.538$). Moreover, the alpha-low gamma PAC was prominent in certain contacts in ACC, it was not uniformly observed across all contacts (Supplementary Fig. S1C, Fig. S2C) although there was an alpha power peak in each contact (Supplementary Fig. S1B, Fig. S2B).

Functional connectivity of alpha oscillations in ACC during LOC

Functional connectivity analysis using coherence approach revealed that in the LOC state a significant increase in coherence of alpha oscillations (7-12 Hz) was observed (p<0.01) between certain left and right contacts in ACC (Fig. 3A, C). In addition, delta oscillations (1.5-4 Hz) in ACC during LOC also exhibited increased coherence compared with awake state (p<0.05). A coherence peak in the alpha band between sensory thalamus and PAG did not appear to change significantly with propofol induction, while there was a coherence increase in a narrow theta band (4.5-7 Hz) in the LOC state (p<0.05) (Fig. 3B, D).

Furthermore, we used the DTF approach to investigate directional influence of driving among the neural activities in different contacts in ACC, with a particular focus on the alpha band. DTF analysis between the LFPs in these contacts in the LOC state showed that the directed flow of alpha band activities from left to right ACC ($DTF_{\text{L1-2}\rightarrow\text{R1-2}} = 0.177$) was stronger than that from right to left ACC ($DTF_{\text{R1-2}\rightarrow\text{L0-1}} = 0.051, DTF_{\text{R1-2}\rightarrow\text{L1-2}} = 0.061$) while there were flows of alpha band activities within left ACC and within right ACC (Fig. 4).

Discussion

This study used the unique opportunity afforded by LFP recording directly from human deep brain structures to characterize the changes of brain activity during induction of LOC using propofol. The main findings are: (1) LOC induced by propofol is accompanied by an increase in alpha power and decrease in gamma power in both cortical and subcortical structures, including ACC, sensory thalamus, and PAG; (2) a distinct temporally dynamic and spatially variable coupling between the phase of alpha oscillations and the amplitude of low gamma oscillations is found in ACC during LOC; (3) the significant coherence in alpha oscillations between specific recording sites in left ACC and right ACC is observed during LOC and there is a bidirectional information flow between left and right ACC but stronger left-to-right flow in the alpha band.

This human study supports the view that activities in multiple cortical and subcortical structures, including cortex and thalamus are affected during anaesthetic-induced unconsciousness [1, 34, 35]. Molecular studies demonstrate that propofol binds postsynaptically to γ-aminobutyric acid type A ($GABA_A$) receptors, hyperpolarizing the postsynaptic neurons thus leading to inhibition [36, 37]. Because GABAergic inhibitory interneurons are widely distributed throughout the cortex, thalamus, brainstem, and spinal cord, propofol induces changes in consciousness through its actions at multiple sites [1, 38]. The phenomena of frequency shifting from beta to alpha band in the transition period and LOC in ACC were consistent with those observed in scalp EEG [6, 39]. Studies of propofol-induced LOC using scalp EEG have shown that alpha oscillations are elevated across the frontal cortices during unconsciousness [6, 40]. Our study showed that the increase of alpha activity was not only concentrated in frontal cortex, but prevalent in multiple deep brain areas, including ACC, sensory thalamus, and PAG. This could be explained in part by recent computational modelling and rat studies that suggest that propofol-induced alpha oscillations is likely due to the modification of the interactions between thalamus and cortex [35, 41, 42]. Moreover, in our study ACC and thalamic oscillations showed significant delta power increase in the LOC state. The increase in delta power in unconsciousness has been hypothesized to be associated with the hyperpolarization of thalamocortical neurons [43]. A recent rat study of coherent delta oscillation between cortex and thalamus during LOC also suggests that propofol-induced delta oscillation involves interactions between cortex and thalamus [35].

We also observed a decreased power in gamma oscillations in both cortical and subcortical structures during LOC, suggesting that it could be a correlate of propofol-induced LOC. Gamma oscillations have been proposed to play important roles in working memory, sensory perception, attention, and motor control. Decreases in gamma power with propofol have been observed in humans using EEG recordings from scalp [8] and ECoG recordings from cortex [9]. Animal studies also found decreased gamma activity in subcortical structures during LOC [44, 45]. Gamma oscillations have been attributed to a variety of underlying functional mechanisms, such as the correlates with the neuronal spiking activity including firing rate and neuronal synchrony [46, 47]. Several studies have revealed that propofol decreases spontaneous neuronal spike rates in both cortex [10, 48] and thalamus [49], suggesting the attenuation of the power in gamma oscillations by propofol likely reflects a decrease of neuronal firing rates [45]. However, other studies found contradictory results of gamma oscillations with propofol [39, 50]. The inconsistent effects of propofol on gamma oscillations might be attributable to the depth of general anaesthesia [44, 48] or dose of anaesthetic [45].

Our findings of increased alpha-gamma PAC in ACC during LOC suggests that PAC could be a possible mechanism for propofol-induced unconsciousness. The modulation of the amplitude of high frequency oscillations by the phase of low frequency oscillations has been implicated as the plausible mechanism for the temporal dynamics and multiregional integration of gamma oscillations [46, 51, 52]. In regard to the interactions between oscillations in anaesthesia, the increased slow wave/delta-gamma PAC and maintained theta-gamma PAC in cortex have been observed in previous human studies of propofol-induced LOC [6, 9]. Recent rat studies also found increased PAC between low frequency (including delta, theta, and alpha bands) oscillations and gamma oscillations in frontal cortex during anaesthetics-induced LOC [19]. Given that decreases in gamma activity and increases in alpha activity appeared during propofol-induced LOC, we speculate that fast oscillating neuronal ensembles in cortex generating gamma activity could be mediated by the emerging slow oscillations of thalamocortical circuits [9], as reflected by the emergence of coupling between the phase of alpha oscillations and the gamma power.

Further, we have highlighted that the PAC in ACC during propofol-induced unconsciousness is spatially variable. In this study, the alpha-gamma PAC was not uniformly observed across all

recording sites in ACC although the increase in alpha power and decrease in gamma power were uniform, suggesting that the regulation of cortical oscillations by propofol in different subregions results from multiple mechanisms. An explanation of this difference may be that gamma oscillations in cortex are generated locally within a few millimeters [53, 54], and the mechanisms of propofol-induced decrease in gamma oscillations generated by different neuronal sources in ACC are different.

Regarding functional connections between regions during anaesthesia, we have shown that the coherence in the alpha band between left and right ACC was increased during unconsciousness, consistent with previous EEG studies showing the increased alpha coherence between frontal brain regions during unconsciousness [7, 55]. Furthermore, directional interhemispheric interactions were found by investigating the directional connectivity of coherent alpha activity between hemispheres. Despite the reciprocal interaction, left to right directionality was stronger. Neuroimaging studies of various cognitive experiments have suggested that hemispheric lateralization is a relative and dynamic phenomenon that depends on specific tasks [56, 57]. A recent functional magnetic resonance imaging study found that propofol conferred differential changes in functional connectivity of the specific and nonspecific thalamocortical systems, particularly in the left hemisphere [58]. We cannot yet give a clear explanation for this hemispheric lateralization during anaesthesia. It is possible that the interaction between cortical hemispheres is an indirect reflection of the thalamocortical interaction and the time delays in propofol-induced alpha oscillations from thalamus to two cortical recording sites are different. The role of hemispheric lateralization in anaesthesia need to be investigated in further studies with task-specific experiments and simultaneous recording of activities in cortex and thalamus.

There are some limitations to this study. First, the number of subjects is relatively small. The paucity of research on deep brain neurophysiology in human related to general anaesthesia reflects the rarity of our data. However such data may provide unique insights into the understanding of anaesthesia-induced unconsciousness. Second, we enrolled patients with chronic pain, and it is possible that the LFP characteristics in several brain regions may be modulated by chronic pain. However, the effects of propofol on brain oscillations here were highly consistent with those observed in healthy subjects and diseased subjects, such as epilepsy

and Parkinson disease [10, 39, 59]. Moreover, individual findings were replicated across subjects despite their individual clinical profiles. The high consistency of these results suggests that the effects reported here are not caused by the presence of pain syndromes but rather reflect a true neural correlate of LOC that is likely to generalize to the healthy brain. Our experiments were within clinical settings in which induction was performed rapidly, causing the transition from consciousness to unconsciousness within 30-100s. This prevented us from correlating the characteristics with the consciousness level. We did not record plasma propofol concentration and thus correlation with propofol level was not possible. However, we characterized the differences of neuronal oscillations between awake and unconsciousness states using several measures, providing robust markers for consciousness, and their dynamic changes over time was achieved by combining these measures and a time-windowing approach. Another limitation is the restricted electrode coverage in each patient, which is determined by clinical need. Thus, our findings should be interpreted only in the context of the cortical and subcortical areas covered. Furthermore, it is still not clear whether the effect of propofol is initiated in thalamus, cortex, or both, and the precise interactions between subcortical and cortical structures and their contributions to the general anaesthesia remain unclear. Given the findings by Flores et al. [35], we suggest that by recording scalp EEG and deep brain LFPs simultaneously, the detection of timing differences in neurophysiological characteristics between subcortical and cortical structures, and their functional connectivity using non-directional and directional measures may help answer these questions.

In conclusion, we report a unique LFPs recording study using multiple human deep brain structures during induction of LOC using propofol. The current work provides neural characteristics associated with LOC reflected by the alterations in alpha power and gamma power in both cortical and subcortical structures and the alpha-gamma PAC in ACC. These findings provide important electrophysiological evidence in humans of different neuronal mechanisms for propofol-induced unconsciousness.

Author Contributions

Y.H., D.W., T.Z.A., and A.L.G. designed the study; Y.H., D.W., N.F.A.B., J.H., S.Y., J.J.F., T.Z.A., and A.L.G. collected the data; Y.H., D.W., S.W., and A.L.G. analysed the data; Y.H., D.W., N.F.A.B., S.W.,

J.H., S.Y., J.J.F., T.Z.A., and A.L.G. wrote and revised the manuscript.

Declaration of Interests

The authors declare no competing interests.

Funding

This work was supported by the NIHR Oxford Biomedical Research Centre, the Charles Wolfson Charitable Trust and the Norman Collisson Foundation.

References

1 Brown EN, Purdon PL, Van Dort CJ. General anesthesia and altered states of arousal: a systems neuroscience analysis. *Annu Rev Neurosci* 2011; **34**: 601-28

2 Fiset P, Paus T, Daloze T, et al. Brain mechanisms of propofol-induced loss of consciousness in humans: a positron emission tomographic study. *J Neurosci* 1999; **19**: 5506-13

3 White NS, Alkire MT. Impaired thalamocortical connectivity in humans during general-anesthetic-induced unconsciousness. *NeuroImage* 2003; **19**: 402-11

4 Boveroux P, Vanhaudenhuyse A, Bruno MA, et al. Breakdown of within- and between-network resting state functional magnetic resonance imaging connectivity during propofol-induced loss of consciousness. *Anesthesiology* 2010; **113**: 1038-53

5 Ni Mhuircheartaigh R, Warnaby C, Rogers R, Jbabdi S, Tracey I. Slow-wave activity saturation and thalamocortical isolation during propofol anesthesia in humans. *Sci Transl Med* 2013; **5**: 208ra148

6 Purdon PL, Pierce ET, Mukamel EA, et al. Electroencephalogram signatures of loss and recovery of consciousness from propofol. *Proc Natl Acad Sci USA* 2013; **110**: E1142-E51

7 Akeju O, Pavone KJ, Westover MB, et al. A comparison of propofol- and dexmedetomidine-induced electroencephalogram dynamics using spectral and coherence analysis. *Anesthesiology* 2014; **121**: 978-89

8 John E, Prichep L, Kox W, et al. Invariant reversible QEEG effects of anesthetics. *Conscious Cogn* 2001; **10**: 165-83

9 Breshears JD, Roland JL, Sharma M, et al. Stable and dynamic cortical electrophysiology of induction and emergence with propofol anesthesia. *Proc Natl Acad Sci USA* 2010; **107**: 21170-5

10 Lewis LD, Weiner VS, Mukamel EA, et al. Rapid fragmentation of neuronal networks at the onset of propofol-induced unconsciousness. *Proc Natl Acad Sci USA* 2012; **109**: E3377-86

11 McCormick DA, Bal T. Sleep and arousal: thalamocortical mechanisms. *Annu Rev Neurosci* 1997; **20**: 185-215

12 Buzsaki G. *Rhythms of the Brain*. Oxford University Press, 2006

13 Goddard CA, Sridharan D, Huguenard JR, Knudsen EI. Gamma oscillations are generated locally in an attention-related midbrain network. *Neuron* 2012; **73**: 567-80

14 Harris KD, Csicsvari J, Hirase H, Dragoi G, Buzsaki G. Organization of cell assemblies in the hippocampus. *Nature* 2003; **424**: 552-6

15 Mukamel EA, Pirondini E, Babadi B, et al. A transition in brain state during propofol-induced unconsciousness. *J Neurosci* 2014; **34**: 839-45

16 Canolty RT, Edwards E, Dalal SS, et al. High gamma power is phase-locked to theta oscillations in human neocortex. *Science* 2006; **313**: 1626-8

17 Fell J, Axmacher N. The role of phase synchronization in memory processes. *Nat Rev Neurosci* 2011; **12**: 105-18

18 Tort AB, Komorowski RW, Manns JR, Kopell NJ, Eichenbaum H. Theta-gamma coupling increases during the learning of item-context associations. *Proc Natl Acad Sci USA* 2009; **106**: 20942-7

19 Pal D, Silverstein BH, Sharba L, et al. Propofol, Sevoflurane, and Ketamine Induce a Reversible Increase in Delta-Gamma and Theta-Gamma Phase-Amplitude Coupling in Frontal Cortex of Rat. *Front Syst Neurosci* 2017; **11**: 41

20 Bittar RG, Kar-Purkayastha I, Owen SL, et al. Deep brain stimulation for pain relief: a meta-analysis. *J Clin Neurosci* 2005; **12**: 515-9

21 Boccard SG, Fitzgerald JJ, Pereira EA, et al. Targeting the affective component of chronic pain: a case series of deep brain stimulation of the anterior cingulate cortex. *Neurosurgery* 2014; **74**: 628-35; discussion 35-7

22 Bokil H, Andrews P, Kulkarni JE, Mehta S, Mitra PP. Chronux: a platform for analyzing neural signals. *J Neurosci Methods* 2010; **192**: 146-51

23 Prerau MJ, Brown RE, Bianchi MT, Ellenbogen JM, Purdon PL. Sleep Neurophysiological Dynamics Through the Lens of Multitaper Spectral Analysis. *Physiology* 2017; **32**: 60-92

24 Baker R, Gent TC, Yang Q, et al. Altered activity in the central medial thalamus precedes changes in the neocortex during transitions into both sleep and propofol anesthesia. *J Neurosci* 2014; **34**: 13326-35

25 Tort AB, Komorowski R, Eichenbaum H, Kopell N. Measuring phase-amplitude coupling between neuronal oscillations of different frequencies. *J Neurophysiol* 2010; **104**: 1195-210

26 Tort AB, Kramer MA, Thorn C, et al. Dynamic cross-frequency couplings of local field potential oscillations in rat striatum and hippocampus during performance of a T-maze task. *Proc Natl Acad Sci USA* 2008; **105**: 20517-22

27 Aru J, Aru J, Priesemann V, et al. Untangling cross-frequency coupling in neuroscience. *Curr Opin Neurobiol* 2015; **31**: 51-61

28 Kaminski MJ, Blinowska KJ. A new method of the description of the information flow in the brain structures. *Biol Cybern* 1991; **65**: 203-10

29 Babiloni F, Cincotti F, Babiloni C, et al. Estimation of the cortical functional connectivity with the multimodal integration of high-resolution EEG and fMRI data by directed transfer function. *NeuroImage* 2005; **24**: 118-31

30 Sharott A, Grosse P, Kuhn AA, et al. Is the synchronization between pallidal and muscle activity in primary dystonia due to peripheral afferance or a motor drive? *Brain* 2008; **131**: 473-84

31 He B, Dai Y, Astolfi L, Babiloni F, Yuan H, Yang L. eConnectome: A MATLAB toolbox for mapping and imaging of brain functional connectivity. *J Neurosci Methods* 2011; **195**: 261-9

32 Theiler J, Eubank S, Longtin A, Galdrikian B, Doyne Farmer J. Testing for nonlinearity in time series: the method of surrogate data. *Physica D* 1992; **58**: 77-94

33 Ding L, Worrell GA, Lagerlund TD, He B. Ictal source analysis: localization and imaging of causal interactions in humans. *NeuroImage* 2007; **34**: 575-86

34 Alkire MT, Hudetz AG, Tononi G. Consciousness and anesthesia. *Science* 2008; **322**: 876-80

35 Flores FJ, Hartnack KE, Fath AB, et al. Thalamocortical synchronization during induction and emergence from propofol-induced unconsciousness. *Proc Natl Acad Sci USA* 2017; **114**: E6660-E8

36 Bai D, Pennefather PS, MacDonald JF, Orser BA. The general anesthetic propofol slows deactivation and desensitization of GABA(A) receptors. *J Neurosci* 1999; **19**: 10635-46

37 Rudolph U, Antkowiak B. Molecular and neuronal substrates for general anaesthetics. *Nat Rev Neurosci* 2004; **5**: 709-20

38 Purdon PL, Sampson A, Pavone KJ, Brown EN. Clinical Electroencephalography for Anesthesiologists: Part I: Background and Basic Signatures. *Anesthesiology* 2015; **123**: 937-60

39 Murphy M, Bruno MA, Riedner BA, et al. Propofol anesthesia and sleep: a high-density EEG study. *Sleep* 2011; **34**: 283-91A

40 Cimenser A, Purdon PL, Pierce ET, et al. Tracking brain states under general anesthesia by using global coherence analysis. *Proc Natl Acad Sci USA* 2011; **108**: 8832-7

41 Ching S, Cimenser A, Purdon PL, Brown EN, Kopell NJ. Thalamocortical model for a propofol-induced alpha-rhythm associated with loss of consciousness. *Proc Natl Acad Sci USA* 2010; **107**: 22665-70

42 Vijayan S, Ching S, Purdon PL, Brown EN, Kopell NJ. Thalamocortical mechanisms for the anteriorization of alpha rhythms during propofol-induced unconsciousness. *J Neurosci* 2013; **33**: 11070-5

43 Alkire MT, Haier RJ, Fallon JH. Toward a unified theory of narcosis: brain imaging evidence for a thalamocortical switch as the neurophysiologic basis of anesthetic-induced unconsciousness. *Conscious Cogn* 2000; **9**: 370-86

44 Ma J, Shen B, Stewart LS, Herrick IA, Leung LS. The septohippocampal system participates in general anesthesia. *J Neurosci* 2002; **22**: RC200

45 Reed SJ, Plourde G. Attenuation of high-frequency (50-200 Hz) thalamocortical EEG rhythms by propofol in rats is more pronounced for the thalamus than for the cortex. *PloS One* 2015; **10**: e0123287

46 Buzsaki G, Wang XJ. Mechanisms of gamma oscillations. *Annu Rev Neurosci* 2012; **35**: 203-25

47 Nir Y, Fisch L, Mukamel R, et al. Coupling between neuronal firing rate, gamma LFP, and BOLD fMRI is related to interneuronal correlations. *Curr Biol* 2007; **17**: 1275-85

48 Ishizawa Y, Ahmed OJ, Patel SR, et al. Dynamics of propofol-induced loss of consciousness across primate neocortex. *J Neurosci* 2016; **36**: 7718-26

49 Ying SW, Goldstein PA. Propofol suppresses synaptic responsiveness of somatosensory relay neurons to excitatory input by potentiating GABA(A) receptor chloride channels. *Mol Pain* 2005; **1**: 2

50 Fell J, Widman G, Rehberg B, Elger CE, Fernandez G. Human mediotemporal EEG characteristics during propofol anesthesia. *Biol Cybern* 2005; **92**: 92-100

51 Buzsaki G, Draguhn A. Neuronal oscillations in cortical networks. *Science* 2004; **304**: 1926-9

52 Jensen O, Colgin LL. Cross-frequency coupling between neuronal oscillations. *Trends Cogn Sci* 2007; **11**: 267-9

53 Sirota A, Montgomery S, Fujisawa S, Isomura Y, Zugaro M, Buzsaki G. Entrainment of neocortical neurons and gamma oscillations by the hippocampal theta rhythm. *Neuron* 2008; **60**: 683-97

54 Wang XJ, Buzsaki G. Gamma oscillation by synaptic inhibition in a hippocampal interneuronal network model. *J Neurosci* 1996; **16**: 6402-13

55 Supp GG, Siegel M, Hipp JF, Engel AK. Cortical hypersynchrony predicts breakdown of sensory processing during loss of consciousness. *Curr Biol* 2011; **21**: 1988-93

56 Jansen A, Menke R, Sommer J, et al. The assessment of hemispheric lateralization in functional MRI--robustness and reproducibility. *NeuroImage* 2006; **33**: 204-17

57 Yang FG, Edens J, Simpson C, Krawczyk DC. Differences in task demands influence the hemispheric lateralization and neural correlates of metaphor. *Brain Lang* 2009; **111**: 114-24

58 Liu X, Lauer KK, Ward BD, Li SJ, Hudetz AG. Differential effects of deep sedation with propofol on the specific and nonspecific thalamocortical systems: a functional magnetic resonance imaging study. *Anesthesiology* 2013; **118**: 59-69

59 Martinez-Simon A, Alegre M, Honorato-Cia C, et al. Effect of Dexmedetomidine and Propofol on Basal Ganglia Activity in Parkinson Disease: A Controlled Clinical Trial. *Anesthesiology* 2017; **126**: 1033-42

Tables and Figures

Table 1. Demographics, etiologies, positions of electrode implantation, and GA induction time.

Subject	Age/Sex	Etiology	Electrode position	Induction time (sec)
1	46/M	Brachial plexus injury	Bilateral ACC	100
2	63/M	Poststroke pain	Bilateral ACC	50
3	53/M	Brachial plexus injury	S Thal PAG	50
4	53/M	Phantom limb pain	S Thal PAG	40
5	39/F	Glossopharyngeal neuralgia	S Thal PAG	90

6	46/M	Phantom limb pain	S Thal	60

ACC, anterior cingulate cortex; S Thal, sensory thalamus; PAG, periaqueductal grey

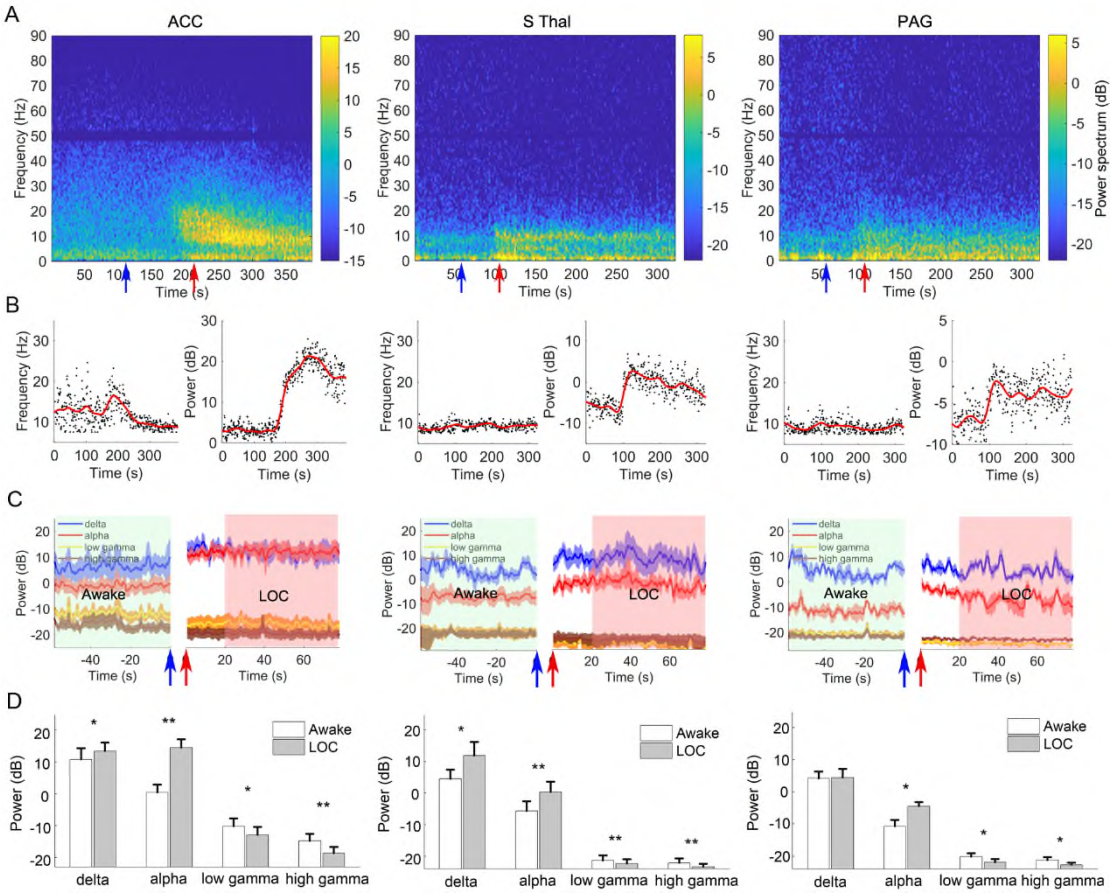

Figure 1. LOC induces an increase in alpha band power and decrease in gamma band power in ACC, sensory thalamus (S Thal, for short), and PAG. (A) Time-frequency representation of the LFPs recorded from ACC, sensory thalamus, and PAG during the induction of GA. The blue arrows indicated the time of propofol injection, and the red arrows indicated the time of loss of eyelash reflex. (B) The changes of peak power and frequency at the peak power between 6 Hz and 40 Hz in the LFPs shown in panel A. (C) Group-level time-variant powers in delta (1-3 Hz), alpha (7-13 Hz), low gamma (30-60 Hz) and high gamma (60-90 Hz) bands of the LFPs recorded from ACC, sensory thalamus, and PAG. The blue arrows indicated the time of propofol injection, and the red arrows indicated the time of loss of eyelash reflex. (D) The statistical analysis of the differences in power in delta, alpha, low gamma and high gamma bands between awake and LOC states in these three regions, respectively. $*$ $p<0.05$; $**$ $p<0.01$.

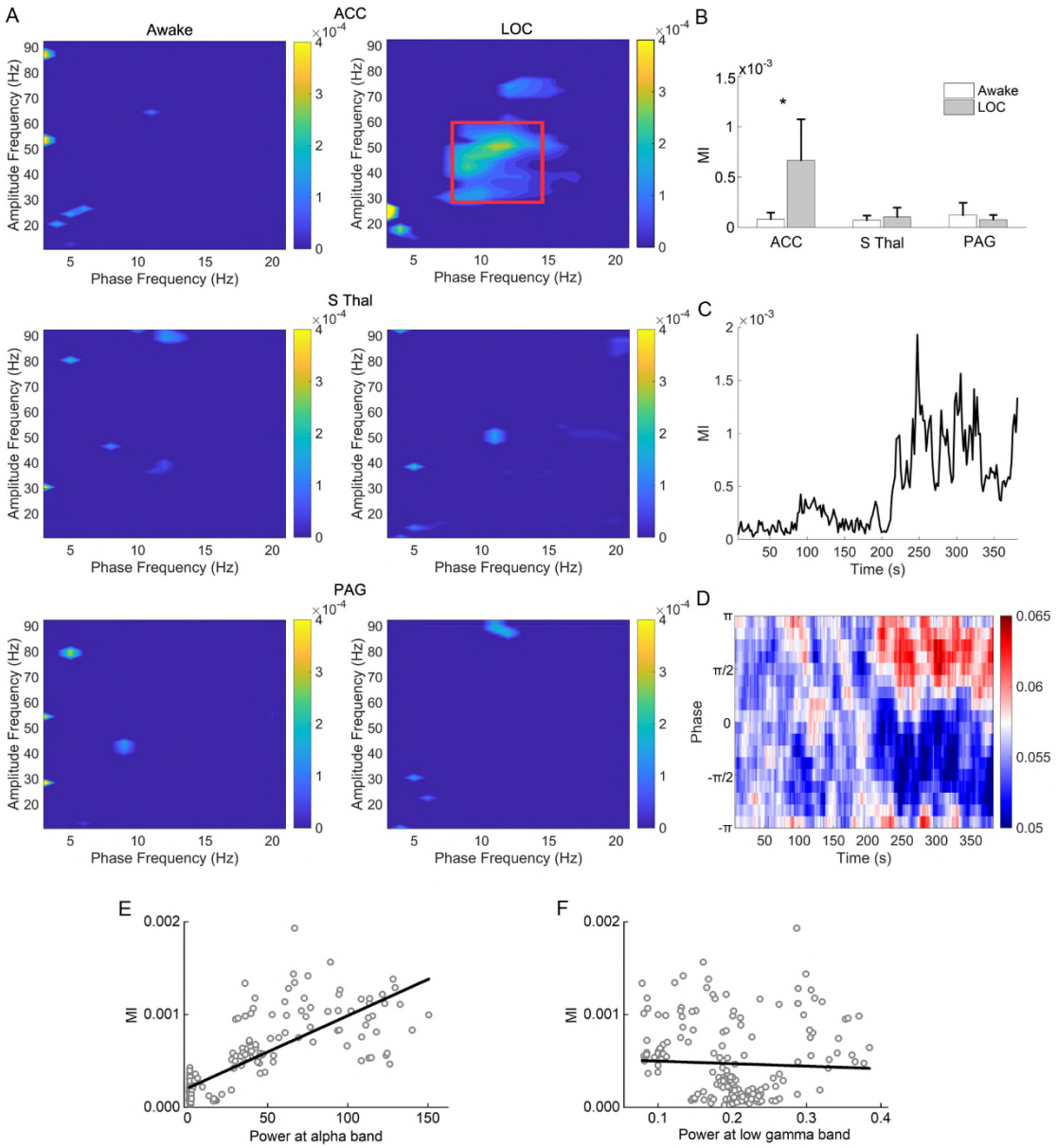

Figure 2. Alpha-low gamma phase-amplitude coupling appears in ACC during LOC state.(A) PAC comodulograms quantified by MI in awake and LOC states in ACC, sensory thalamus (S Thal, for short), and PAG, respectively. (B) The group statistical analysis of the differences in alpha-low gamma PAC between awake and LOC states in these three regions, respectively. $\star$ p<0.05. (C) The time-variant alpha-low gamma PAC in the contacts in ACC shown in panel A. (D) The time-variant phase-amplitude histogram showing the relationship between the alpha phase (y-axis) and low gamma amplitude (color map) in the same contacts as in panel C. (E) The correlation between the time-variant alpha-low gamma PAC and alpha power in ACC. (F) The correlation between the time-variant alpha-low gamma PAC and low gamma power in ACC.

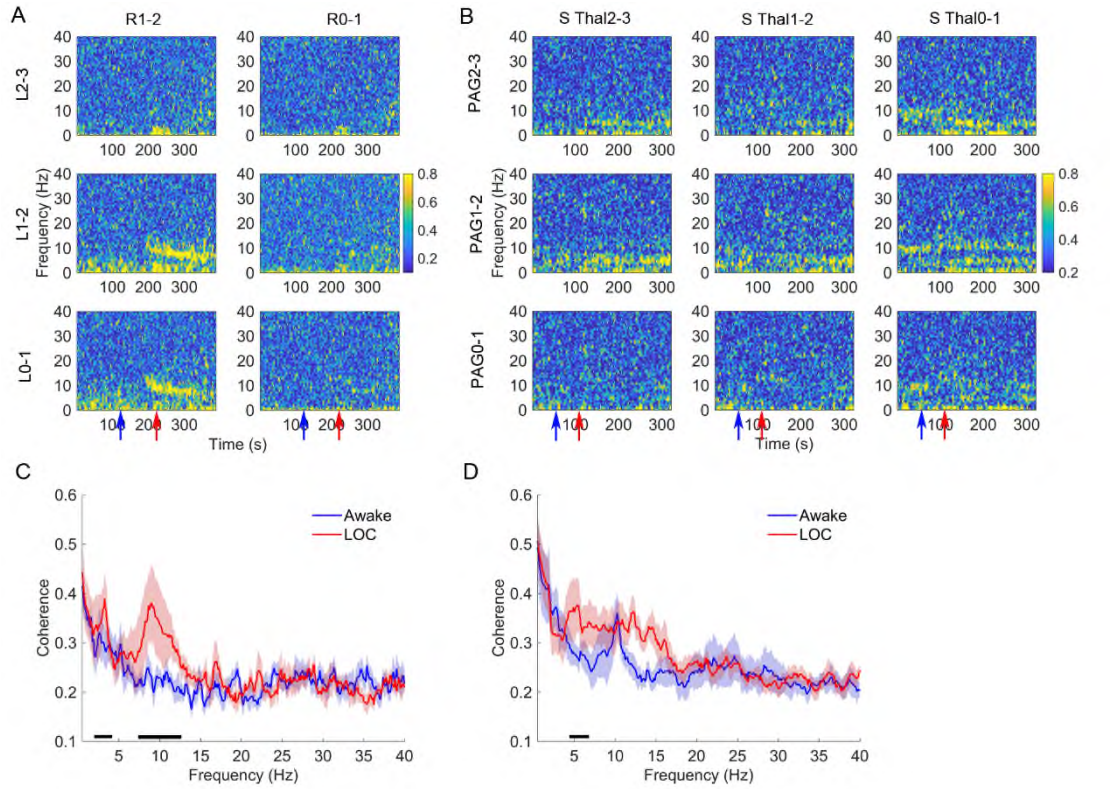

Figure 3. Alpha oscillations in the left and right ACC are coherent during LOC. (A) The time-variant coherence representation of the LFPs between the contacts in left (rows) and right (columns) ACC (L indicates left ACC and R indicates right ACC, channel R2-3 in this subject was excluded from analysis). The blue arrows indicated the time of propofol injection, and the red arrows indicated the time of loss of eyelash reflex. (B) The time-variant coherence representation of the LFPs between the contacts in sensory thalamus (rows) and PAG (columns). The blue arrows indicated the time of propofol injection, and the red arrows indicated the time of loss of eyelash reflex. (C) The statistical analysis of the coherence between left and right ACC in awake state versus in LOC state. (D) The statistical analysis of the coherence between sensory thalamus and PAG in awake state versus in LOC state. Horizontal solid black line indicates frequency ranges at which significant difference existed (p<0.05).

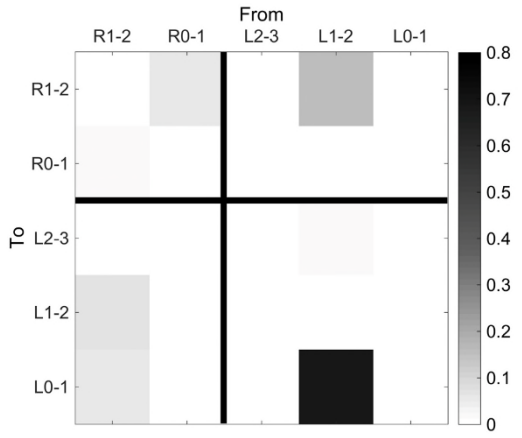

Figure 4. Alpha DTF between the contacts in ACC in the LOC state (L indicates left ACC and R

indicates right ACC, channel R2-3 in this subject was excluded from analysis).